Eur. Phys. J. E (2018) **41**: 108
DOI 10.1140/epje/i2018-11714-8

THE EUROPEAN PHYSICAL JOURNAL E

Regular Article

Unique dynamic crossover in supercooled x,3-dihydroxypropyl acrylate (x = 1, 2) isomers mixture

Szymon Starzonek[1,3,a], Aleksandra Kędzierska-Sar[1,2], Aleksandra Drozd-Rzoska[1,3], Mikołaj Szafran[2], and Sylwester J. Rzoska[1,3]

[1] Institute of High Pressure Physics, Polish Academy of Sciences, ul. Sokołowska 29/37, 01-142 Warsaw, Poland
[2] Department of Chemical Technology, Warsaw University of Technology, ul. Noakowskiego 3, 00-664 Warsaw, Poland
[3] Warsaw Dielectrics Group, Warsaw, Poland

Received 15 August 2017 and Received in final form 6 July 2018
Published online: 20 September 2018

Abstract. The previtreous dynamics in the glass-forming monomer, glycerol monoacrylate (GMA), was tested using the broadband dielectric spectroscopy (BDS). The measurements revealed a clear dynamic crossover at the temperature $T_B = 254\,\mathrm{K}$ and the time scale $\tau(T_B) = 5.4\,\mathrm{ns}$ for the primary (structural) relaxation time and no hallmarks for the crossover for the DC electric conductivity σ_{DC}. This result was revealed via the derivative-based and distortions-sensitive analysis $\mathrm{d}\ln H_a/\mathrm{d}(1/T)$ *vs.* $1/T$, where H_a stands for the apparent activation energy. Subsequent tests of the fractional Debye-Stokes-Einsten relation $\sigma_{DC}(\tau_\alpha)^S = \mathrm{const}$ showed that the crossover is associated with $S = 1$ (for $T > T_B$) $\rightarrow$ $S = 0.84$ (for $T < T_B$). The crossover coexists with the emergence of the secondary beta relaxation, which smoothly develops deeply into the solid amorphous phase below the glass temperature T_g.

1 Introduction

One of the most mysterious forms of the solidification is the vitrification at the glass temperature when passing from the metastable ultraviscous liquid/fluid to the metastable amorphous solid glass state [1]. Although the glass temperature T_g cannot be directly determined because of its puzzling nature, it is associated with far previtreous effects signaling the vitrification even 100 K above T_g. This inherent feature allows for the "remote" estimation of the T_g value. Regarding the previtreous "dynamic effects" one can recall such "universal-like" behavior as i) the non-Arrhenius evolution on the primary relaxation time (τ), viscosity (η) or electric conductivity (σ), ii) the non-Debye distribution of the relaxation time, iii) the dynamic crossover between the ergodic and non-ergodic dynamical regimes, most often associated with the time scale $\tau_B = 10^{-7\pm1}\,\mathrm{s}$, iv) the emergence of the secondary relaxation in the ultraslowing domain for $T < T_B = T(\tau = \tau_B)$. The glass temperature is by convention associated with the time scale of the primary relaxation process, $\tau(T_g) = 100\,\mathrm{s}$ which corresponds to the empirically observed T_g value in the heat capacity scan for the most standard cooling rate $10\,\mathrm{K}\cdot\mathrm{min}^{-1}$ [2,3]. The fascinating previtreous "universal-like" behavior of the dynamic properties on approaching the glass temperature is undoubtedly one of the key reasons why the problem of in-depth fundamental understanding of the glass transition is indicated as one of the greatest challenges for the 21st century condensed matter physics, with an enormous importance for the material engineering implementations [1–4]. One of the issues in this domain, which may appear essential for the ultimate insight, is the lack of studies covering domains on both sides of the glass transition, *i.e.* the metastable ultraviscous liquid and the metastable amorphous solid. In fact conclusive research on the latter is particularly difficult due to the fact that when passing the time scale $\tau(T_g)$ the system time scale exceeds the experimental one by decades, making ultimate conclusions challenging [2,3].

In this report it is shown that the secondary relaxation process [1–3], several decades faster than the primary relaxation time, seems to continue smoothly deeply within the solid glass state. Its evolution in this solid state clearly correlates with such basic feature of the liquid state as the dynamic crossover. Studies were carried out in the glycerol monoacrylate monomeric system, which is important for application in ceramics formation.

2 Experimental

The tested glass former was glycerol monoacrylate, which is a low-toxicity monomer used for manufacturing ceramic materials through the gelcasting process [5–7]. The

[a] e-mail: starzoneks@unipress.waw.pl

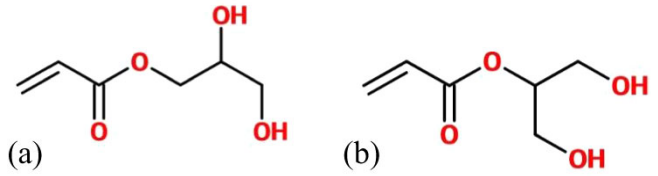

Fig. 1. Molecular structures of 2,3-dihydroxypropyl acrylate (a) and 1,3-dihydroxypropyl acrylate (b).

monomer, present in the ceramic slurry, polymerizes during the forming process inside the mold.

The tested sample was composed by 2,3-dihydroxypropyl acrylate (70% wt.) and 1,3-dihydroxypropyl acrylate (30% wt.). Their molecular structures are shown in fig. 1. GMA was synthesized at the Warsaw University of Technology. It has a number of advantages when compared to different commercial monomers. It is water soluble, which allows conducting the process in water. Due to the presence of two –OH groups, the use of a crosslinking agent is not necessary.

The complex dielectric permittivity $\varepsilon^*(f) = \varepsilon'(f) - i\varepsilon''(f)$ and electric conductivity $\sigma(f)$ were measured using the Alpha-A impedance analyzer (Novocontrol) with 6-digits resolution at ambient pressure ($P = 0.1$ MPa) over a frequency range from 10^7 Hz to 1 Hz. During measurements the sample was maintained under a nitrogen gas flow in a temperature range between 273 K and 143 K. The temperature was controlled using Quatro Cryosystem (Novocontrol) with stability better than $\Delta T = 0.1$ K. The liquid GMA was put into a two-round-parallel-plates measurement capacitor made of steel with diameter $2r = 20$ mm. A Teflon® ring was used as a spacer yielding a macroscopic gap $d = 0.2$ mm. The dielectric loss spectrum gives a background for the relaxation times analysis $\tau = (2\pi f)^{-1}$, where f is the frequency of the peak's maximum, and DC-conductivity σ_{DC}; however in this paper all dielectric spectra were fitted using Havrilliak-Negami function $\varepsilon^*(\omega) = \varepsilon_\infty + \frac{\Delta\varepsilon}{(1+(i\omega\tau)^\alpha)^\beta}$, where ε_∞ is the permittivity at the high-frequency limit, $\Delta\varepsilon = \varepsilon_\infty - \varepsilon_s$, τ is the characteristic relaxation time of the system, the exponents α and β describe the asymmetry and broadness of the corresponding spectra [1–3].

3 The evolution of relaxation times and the dynamic crossover

One of the key features of the glass previtreous dynamics is the super-Arrhenius behavior of the primary (α, *alpha*) relaxation time [1–4]:

$$\tau(T) = \tau_0 \exp\left(\frac{E_A(T)}{RT}\right), \tag{1}$$

where $E_A(T)$ stands for the apparent activation energy. This relation converts into the classical Arrhenius dependence when in the given temperature domain $E_A(T) = E_A = \text{const}$.

The generally unknown form of the evolution of the apparent activation energy causes that in the portrayal of experimental data one has to use ersatz dependences. For decades the most popular was the Vogel-Fulcher-Tammann (VFT) dependence [1–4,8–10]:

$$\tau(T) = \tau_0 \exp\left(\frac{D_T T_0}{T - T_0}\right), \tag{2}$$

where D_T denotes the fragility strength coefficient, T_0 is for the ideal glass "transition" temperature hidden in the solid glassy state. By comparing eqs. (1) and (2) for the apparent activation energy the following equation has been obtained: $E_A(T) = RD_T/(T_0^{-1} - T^{-1})$.

In recent years, novel equations yielding more optimal $\tau_\alpha(T)$ or $\eta(T)$ parameterizations and questioning the general validity of the VFT relation appeared [11–18]. Particularly successful appears the relation empirically introduced by Waterton [19] in 1932 and recently validated as the output of the constraint theory applied to the Adam-Gibbs model by Mauro *et al.* [13] (MYEGA) namely

$$\tau(T) = \tau_0 \exp\left[\frac{K}{T} \exp\left(\frac{C}{T}\right)\right]. \tag{3}$$

It is notable that it has no finite-temperature divergence, which is the characteristic feature of the VFT relation. Nevertheless, the ultimate parameterization of the temperature dependence of the primary relaxation or viscosity in the ultraviscous domain remains a puzzling issue. Worth recalling here is the recent "model-free" ("fitting-free") analysis based on the apparent activation temperature index, which clearly shows the limited fundamental validity of all basic equations used so far, including the VFT and WM (MYEGA) ones.

One of the "universal-like" behaviours of the previtreous dynamics is the change in the form of the super-Arrhenius (SA) behavior most often occurring at the "magic" time scale $\tau(T_B) \sim 0.1\,\mu$s, although there is also a notable number of exceptions [2,20]. The key tool for the detection of the crossover is the plot proposed two decades ago by Stickel *et al.* [21]: $\phi_T(T) = [\mathrm{d}\log_{10}\tau_\alpha(T)/\mathrm{d}(1/T)]^{-0.5}$ *vs.* $1/T$. As shown in refs. [11, 12] this plot is related to the evolution of the apparent activation enthalpy with the underlying background of the hypothetical general validity of the VFT equation, namely

$$\phi_T(T) = (H_A(T))^{-0.5} = A - \frac{B}{T}, \tag{4}$$

where the apparent activation energy $H_A(T) = R\frac{\mathrm{d}\ln\tau_\alpha(T)}{\mathrm{d}(1/T)}$. Note that $\ln\tau_\alpha = \log_{10}\tau_\alpha/\log_{10}e$. The "linearization-focused" transformation of the experimental data via eq. (4) enables the unequivocal estimation of the basic parameters in the VFT equation: $T_0 = |B/A|$, $D_T = 1/|AB|$.

Regarding the significance of the dynamic crossover phenomenon worth recalling is the statement from ref. [22]: "*... one may expect that understanding the meaning of the dynamic crossover phenomenon may be*

essential for the ultimate understanding of the puzzling nature of the glass transition. ... T_B appears to be more relevant than T_g or T_0 ...".

It is notable that the estimation of the location of T_B via the "Stickel plot" or eq. (4) assumes the fundamental validity of the VFT description for the super-Arrhenius evolution of the primary relaxation time or related properties. However, as shown in refs. [16–18] this is the case only for a limited number of glass formers. Consequently, the question arises for the "fitting-free" way determining of the dynamical crossover. In refs. [16–18] it was noted that the domain of validity of the MYEGA equation (3) can be estimated via the following derivative-based and distortions-sensitive plot based on $\tau_\alpha(T)$ experimental data: $\ln[H'_A/(1+C/T)]$ *vs.* $1/T$ [23]. The linear plot indicates the validity domain of such description and the subsequent linear regression fit yield optimal values of the basic parameters in eq. (3). Following this result, in refs. [11,12] the new "model-free"/"fitting-free" way of analysis indicating changes in the form of description of $\tau_\alpha(T)$ behavior was proposed and tested for several glass-forming systems: $\ln(H_A(T)/R)$ *vs.* $1/T$, where the apparent activation enthalpy $H_A(T) = \mathrm{d}\ln\tau_\alpha/\mathrm{d}(1/T)$.

Another possibility of the "fitting-free" way is the analysis focused on the emergence of the orientational-translational decoupling in the non-ergodic domain below T_B [2,3]. For BDS related experimental data it is expressed via the fractional Debye-Stokes-Einstein relation:

$$(\sigma_{DC}(T))\,(\tau_\alpha(T))^S = \text{const [24]}. \tag{5}$$

The value of the exponent $S < 1$ is expected for $T_g < T < T_B$ and indicates the orientational-transitional decoupling, *i.e.* the speed-up of orientational processes in comparison with translational ones. For $T > T_B$ the exponent $S = 1$ and both processes are coupled, *i.e.* the time scale of orientational and translational dynamics appear paralleled coupled. Most liquids are characterized by $0.7 < S < 1$ [24]. However, in some liquid crystal's phases the exponent can be even smaller than 0.5 [25,26]. In ref. [24] the link of the exponent S to the activation enthalpy of the process was shown.

One of "universal-like" features of the previtreous dynamic is the emergence of the secondary, "beta" (β), relaxation process for $T < T_B$. Both "alpha" and "beta" relaxation processes split at $T = T_B$ and when reaching T_g the difference between the related time scale reaches several decades. It is notable that the secondary relaxation most often follows the Arrhenius pattern. In the case of polymeric glass formers the beta relaxation is linked to internal molecular relaxation processes [2,3].

4 Results and discussion

Figure 2 presents examples of dielectric loss spectra $\varepsilon''(f)$ for supercooled GMA samples when decreasing temperatures from 273 K to 193 K. The emergence of weak primary (structural) relaxation τ_α, deep-glassy process β and

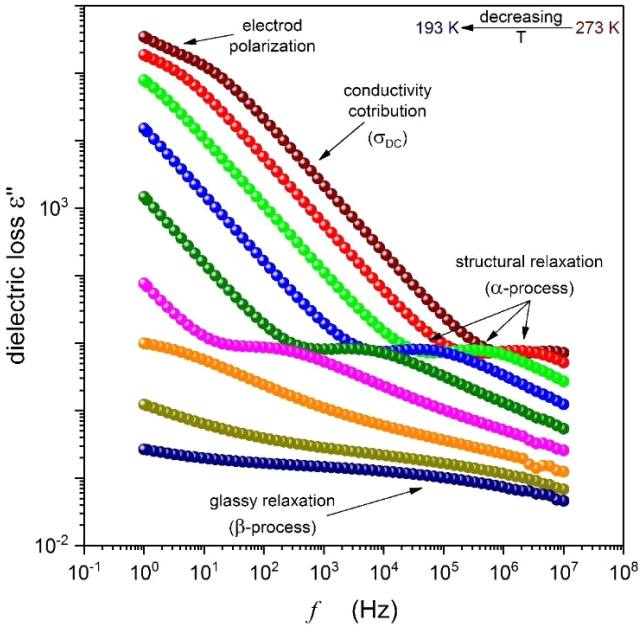

Fig. 2. Dielectric loss spectra $\varepsilon''(f)$ for glycerol monoacrylate mixture at decreasing temperature from 273 K down to 193 K. The two relaxation processes: structural (α) and glassy (β); and conductivity contribution σ_{DC} are presented.

strong conductivity contribution is visible. The characteristic slope change of the low-frequency part of the spectra at the $\log_{10}\varepsilon''$ *vs.* $\log_{10} f$ plot is related to the electrode polarization appearing in highly conductive systems, to which GMA belongs. This low-frequency part of the spectra also serves for determining the DC-conductivity. Regarding the basic structural α-process, dielectric loss curves exhibit a non-Debye shape, typical for complex glassy dynamics. The obtained evolution of relaxation times is presented in fig. 3(a), covering both the ultraviscous liquid and solid states. Figure 3(b) shows results of the supplementary distortions-sensitive and derivative-based analysis of the data, following the method recalled in the previous section.

The horizontal solid line (red) indicates the behavior well portrayed by the simple Arrhenius relation, eq. (1). It is associated with the activation energy $E_A = 27\,\mathrm{kJ\cdot mol^{-1}}$. On cooling there is an almost 100 K broad super-Arrhenius domain, which can be well portrayed by the VFT equation (2): $T_0 = 159.10\,\mathrm{K}$, $D_T = 10.15$. Due to the VFT behavior one can obtain the fragility index m, which is a measure of deviation from the Arrhenius behavior ($m = 1$). It is possible to estimate the value of the fragility coefficient, using the formula $m = m_{P=0.1\,\mathrm{MPa}} \approx 16 + 590/D_T$, given by Boehmer *et al.*, for $m = [\mathrm{d}\log_{10}\tau_\alpha/\mathrm{d}(T_g/T)]_{T\to T_g}$ [2,3]. For the studied system $m = 76$. Notable is the very clear appearance of the dynamic crossover at $T_B = 254\,\mathrm{K}$, for the relaxation time $\tau_\alpha(T_B) = 5.4\,\mathrm{ns}$.

Translational processes are characterized within the BDS spectrum by the DC electric conductivity. Its temperature evolution within the ultraviscous liquid state is shown in fig. 4(a), revealing a clear super-Arrhenius

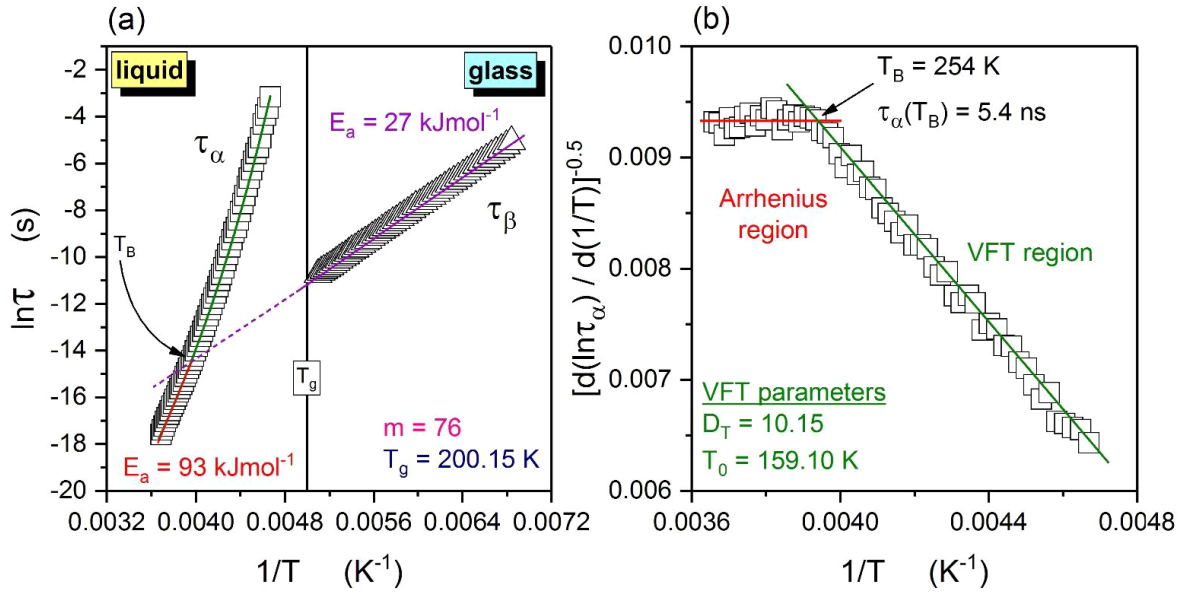

Fig. 3. (a) Distribution of relaxation times: primary (α) and secondary (β) for a liquid and glassy glycerol monoacrylate mixture. The solid vertical line presents the glass transition temperature $T_g = 200.15\,\mathrm{K}$. From the Arrhenius behaviors of relaxation times activation energies were calculated. (b) Derivative-based analysis of the structural relaxation time (α), the so-called "Stickel plot". This linearization allows to obtain dynamic regions by decreasing the temperature and calculate VFT parameters, which can be used for estimating the fragility index $m = 76$. The dynamic crossover occurs at a temperature $T_B = 254\,\mathrm{K}$ and the relaxation time in this point $\tau_\alpha(T_B) = 5.4\,\mathrm{ns}$.

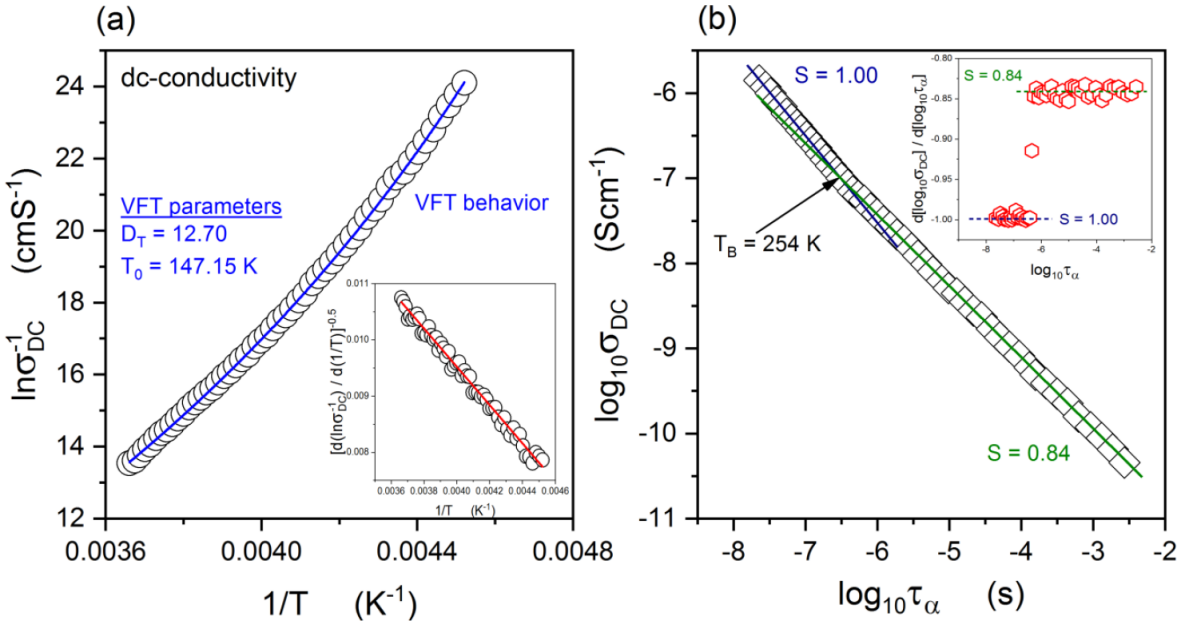

Fig. 4. (a) The VFT behavior of the DC-conductivity reciprocal. (b) The fractional Debye-Stokes-Einstein test. At lower temperatures the transitional-orientational decoupling occurs. The inset shows the derivative analysis with two characteristics values of the FDSE exponent, which have different slopes: $S = 1.0$ for the super-Arrhenius region, and $S = 0.84$ for the VFT domain.

behavior. The distortion-sensitive and derivative-based plot $(\mathrm{d}\ln\sigma_{DC}^{-1}/\mathrm{d}(1/T))^{-0.5}$ *vs.* $1/T$ shows no hallmarks of the translational-orientational decoupling for the electric conductivity when passing T_B, clearly manifested in the $\tau_\alpha(T)$ evolution. The dynamic crossover is present, while testing the orientational processes and absent for translational ones. The evolution of $\sigma_{DC}^{-1}(T)$ is well portrayed by elation (the solid curve in fig. 4(a)) and it is associated with the fragility index $m_\sigma = 64.45$.

The translational-orientational (TO) coupling/decoupling is directly tested in fig. 4(b) via the test of the validity of the Debye-Stokes-Einstein. The inset shows the derivative of $\mathrm{d}\log_{10}\sigma_{DC}/\mathrm{d}\log_{10}\tau_\alpha$ of data from the main part of the plot, conforming the occurrence of the dynamic crossover at the well-defined temperature T_B, the same as in fig. 3. The crossover is associated with the shift from the region of obeying the DSE law and the translational-orientational coupling ($S = 1$) to the decoupling region ($S = 0.84$) in the immediate vicinity of T_g. It was derived in ref. [24] that the fractional DSE exponent

$$S = \frac{H_A^{\sigma_{DC}}}{H_A^{\tau_\alpha}} = \frac{m^{\sigma_{DC}}}{m^{\tau_\alpha}}, \quad (\text{for } P = \text{const}), \tag{6}$$

where $H_A^{\sigma_{DC}}$, $H_A^{\tau_\alpha}$ are apparent activation enthalpies and $m^{\sigma_{DC}}$, m^{τ_α} are "fragility indexes" calculated from DC-conductivity and structural relaxation data, respectively. For glycerol monoacrylate (GMA) the exponent $S = 0.84$ is in fair agreements with the value $S = m^{\sigma_{DC}}/m^{\tau_\alpha} = 64.45/76 \approx 0.848$.

The common, "universal-like" feature of the dynamics in the non-ergodic domain closed to T_g is the emergence of a secondary relaxation process. This is also the case of GMA dynamics. However, this process becomes particularly well visible in the solid amorphous state, for $T < T_g$. The detection of this beta process in the solid amorphous phase is easily possible even 50 K below T_g, where $\tau_\beta(T_g - 50\,\mathrm{K}) \sim 10^{-4}\,\mathrm{s}$, *i.e.* it is experimentally detectable. The direct detection of the structural relaxation time τ_α for such temperature is in practice not possible, because it approximately exceeds a millions of years value.

5 Conclusions

This report present the analysis of the dynamics in a glycerol monoacrylate (GMA) mixture, being the glass former important in the gelcasting technology in ceramics. The tested system shows relatively high electric conductivity, but despite this difficulty the broadband dielectric scanning enabled tests of the temperature evolution of the orientational and translational relaxation processes. The structural relaxation time $\tau_\alpha(T)$ shows a clear dynamic crossover from the Arrhenius to super-Arrhenius behavior at the temperature $T_B \approx 254\,\mathrm{K}$. The crossover is absent for the DC electric conductivity, related to translational processes. The crossover is clearly visible also in tests focused on the occurrence of the fractional Debye-Stokes-Einstein law. In the solid amorphous state the primary relaxation time $\tau_\alpha(T)$ ceases to be directly detectable due to the enormous increasing of the system time scale. Nevertheless, there is a clear manifestation of the qualitatively faster relaxation process, which after the extrapolation to the ultraviscous liquid state merges with the structural relaxation time at $T = T_B$, which allows to assume that for the given system the secondary relaxation processes smoothly develop from the metastable ultraviscous liquid state to the metastable solid glass state without a hallmark when passing the solidification point at the glass temperature.

For some of the authors (SS, SJR, ADR) the research was supported by the NCN OPUS (Poland) Project ref. 2016/21/B/ST3/02203 (UMO-2016/21/B/ST3/02203). For AKS this work was financed from the National Science Centre in Poland from grant number 2014/13/N/ST5/03438.

Author contribution statement

Characterization and the temperature scans of dielectric permittivities were carried out by SS and AKS. Data was analysed by SS, ADR and SJR. Key issues of the paper were formulated and written by SS, AKS and SJR with discussing impact of MS.

References

1. D. Kennedy, Science **309**, 83 (2005).
2. S.J. Rzoska, V. Mazur (Editors), *Soft Matter under Exogenic Impacts*, NATO Sci. Ser. II, Vol. **242** (Springer, Berlin, 2007).
3. K.L. Ngai, *Relaxation and Diffusion in Complex Systems* (Springer, Berlin, 2011).
4. L. Berthier, M.D. Ediger, Phys. Today **69**, 40 (2016) issue No. 1.
5. G. Tari, Am. Ceram. Soc. Bull. **82**, 43 (2003).
6. C. Tallón, R. Moreno, M.I. Nieto, D. Jach, G. Rokicki, M. Szafran, J. Am. Ceram. Soc. **90**, 1386 (2007).
7. C. Tallon, D. Jach, R. Moreno, M.I. Nieto, G. Rokicki, M. Szafran, J. Eur. Ceram. Soc. **29**, 875 (2009).
8. H. Vogel, Phys. Z. **22**, 645 (1921).
9. G.S. Fulcher, J. Am. Chem. Soc. **8**, 339 (1925).
10. G. Tammann, W. Hesse, Z. Anorg. Allg. Chem. **15**, 245 (1926).
11. J.C. Martinez Garcia, J.Ll. Tamarit, S.J. Rzoska, J. Chem. Phys. **134**, 024512 (2011).
12. J.C. Martinez-Garcia, J. Martinez-Garcia, S.J. Rzoska, J. Hulliger, J. Chem. Phys. **137**, 064501 (2012).
13. J.C. Mauro, Y. Yue, A.J. Ellison, P.K. Gupta, D.C. Allan, Proc. Natl. Acad. Sci. U.S.A. **106**, 19780 (2009).
14. P. Lunkenheimer, S. Kastner, M. Köhler, A. Loidl, Phys. Rev. E **81**, 051504 (2010).

15. T. Hecksher, A.I. Nielsen, N.B. Olsen, J.C. Dyre, Nat. Phys. **4**, 737 (2008).
16. J.C. Martinez-Garcia, S.J. Rzoska, A. Drozd-Rzoska, J. Martinez-Garcia, Nat. Commun. **4**, 1823 (2013).
17. J.C. Martinez-Garcia, S.J. Rzoska, A. Drozd-Rzoska, J. Martinez-Garcia, J.C. Mauro, Sci. Rep. **4**, 5160 (2014).
18. J.C. Martinez-Garcia, S.J. Rzoska, A. Drozd-Rzoska, S. Starzonek, J.C. Mauro, Sci. Rep. **5**, 8314 (2015).
19. S.C. Waterton, J. Soc. Glass Technol. **16**, 244 (1932).
20. V.N. Novikov, A.P. Sokolov, Phys. Rev. E **67**, 031507 (2003).
21. F. Stickel, E.W. Fischer, R. Richert, J. Chem. Phys. **102**, 6251 (1995).
22. F. Mallamace, C. Branca, C. Corsaro, N. Leone, J. Spooren, S.-H. Chen, H.E. Stanley, Proc. Natl. Acad. Sci. U.S.A. **107**, 22457 (2010).
23. A. Drozd-Rzoska, S.J. Rzoska, C.M. Roland, J. Phys.: Condens. Matter **20**, 244103 (2008).
24. S. Starzonek, S.J. Rzoska, A. Drozd-Rzoska, S. Pawlus, E. Biała, J.C. Martinez-Garcia, L. Kistersky, Soft Matter **11**, 5554 (2015).
25. M. Głuszek, A. Antosik, M. Szafran, S.J. Rzoska, M. Zalewski, E. Pawlikowska, S. Starzonek, J. Non-Cryst. Solids **471**, 91 (2017).
26. S. Starzonek, S.J. Rzoska, A. Drozd-Rzoska, K. Czupryński, S. Kralj, Phys. Rev. E **96**, 022705 (2017).